2006

Investigation of Transient Two-Phase Flow During Refrigeration and Air Conditioning System Startup

Michael J. Hedrick
University of Illinois at Urbana-Champaign

Emad W. Jassim
University of Illinois at Urbana-Champaign

Ty A. Newell
University of Illinois at Urbana-Champaign

Investigation of Transient Two-Phase Flow During Refrigeration and Air Conditioning System Startup

Michael J. Hedrick[1], Emad W. Jassim[2], Ty A. Newell[3]

University of Illinois
Department of Mechanical and Industrial Engineering
1206 W. Green St.
Urbana, IL 61801

[1] Graduate Assistant
Phone: 309.645.5575 Fax: 217.333.1942 Email: hedrick2@uiuc.edu

[2] Graduate Assistant
Phone: 309.377.8249 Fax: 217.333.1942 Email: jassim@uiuc.edu

[3] Professor of Mechanical Engineering
Phone: 309.377.8249 Fax: 217.333.1942 Email: tynewell@uiuc.edu

ABSTRACT

The characteristics of transient two-phase refrigerant flow, specifically slug flow, related to air conditioning and refrigeration system startup conditions are investigated. The apparatus used to collect information necessary for modeling slug motion is described. Flow visualization techniques and implementation of optical film thickness sensors are described. Important physical trends of the flow for an air/water system are discussed using flow visualization images and experimental data. Analytical models describing slug motion for an air/water system are developed. These models are applied to the experimental data. Their effectiveness in predicting the transient slug motion are analyzed and compared.

1. INTRODUCTION

The ability to predict the distribution of refrigeration charge under steady state conditions has been improving as more two-phase steady state research is being conducted. However, little information can be found in the literature concerning transient two-phase flow, which exists during startup conditions in vapor compression systems. When a refrigeration system is shut down, the refrigerant vapor condenses and pools in either the high or low pressure side of the system. This liquid mass is accelerated through the system as a result of the high side pressure increase from compressor startup.

The refrigerant slug motion is expected to be quite different on the high and low sides of a system. A slug on the high side would tend to remain at a subcooled liquid due to the increase in high side pressure during startup. This mass would then be accelerated towards a receiver or an expansion device. On the low side, the pressure is reduced during startup, possibly below the refrigerant saturation pressure. This would cause nucleation of refrigerant vapor bubbles, having a previously uninvestigated effect on the motion or dissipation of the slug.

Liquid slugs in both circumstances create undesirable effects such as damage to system components, undesirable noises, and delay in the establishment of steady state conditions. This investigation attempts to describe the motion of the liquid slug and the conditions during which the slug dissipation or break down. Once the refrigerant slug can

be accurately modeled, steps can be taken to minimize the damage to components or better approach the other problems.

All analyses herein have been derived from experimentation with air/water systems. Air/water was chosen as the working fluid for this investigation in order to easily develop an experimental apparatus and analytical models without the complication of evaporation or condensation described above. Future testing will include common refrigerants (such as R134a) and models of slug motion will be modified to accommodate additional physical phenomena.

2. TEST APPARATUS

2.1 Test Section

A once through refrigerant loop was set up in order to study the slug motion. The apparatus consists of a high pressure source, a low pressure source, 5 meter transparent PVC pipe section, 2 pressure transducers, and 11 film thickness sensors. The apparatus is shown in Figure 1.

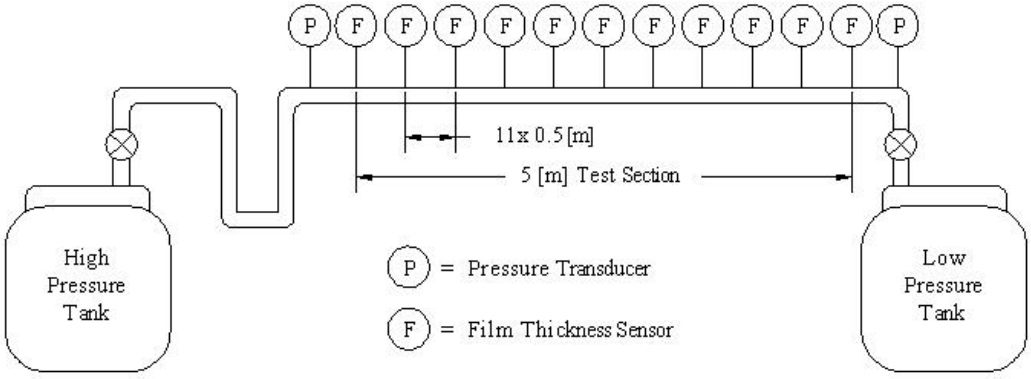

Figure 1: Test Section Schematic

Because the working fluid is air/water, the high and low pressure tanks are substituted for dry, high pressure supply air at approximately 690 kilopascals and a drain at atmospheric pressure, respectively. A pressure regulator is added immediately after the high pressure valve in order to control the magnitude of the driving pressure difference. A u-shaped section (shown on the left side of Figure 1) is used to collect known volumes of water to generate a slug prior to the application of the high pressure air. The film thickness sensors are located on the bottom of the test section.

Tests were conducted with air/water varying the following parameters:

- Slug volume: 100-400 [mL]
- High side pressure: 69-276 [kPa]
- Low side valve: open, closed

The tests were conducted on a 10.2 millimeter inner diameter transparent PVC pipe. Other pipe sizes, pipe orientations, and working fluids will be investigated in future experiments. High side pressure, low side pressure, and film thickness data from the 11 sensors are recorded for each test. Flow visualization videos are also taken at each test condition.

2.2 Flow Visualization Images

A standard web-cam and stroboscope are used to record video images of the flow. The stroboscope, in addition to projecting a sheet of alternating black and white stripes, increases the quality of the images. The contrasting strips simplify identification of liquid vapor interfaces (Jassim 2006).

This flow visualization method is not completely effective for transient testing of this type, however. The frame rate of the camera limits the recordable speed to approximately 1.8 meters per second. During a significant portion of

the test, the fluid phenomena occur at speeds higher than the camera limit. Characteristics like the leading and trailing profile of the slug can not be recorded. A high speed camera will be used to record data as it becomes available.

2.3 Film Thickness Sensors

Optical film thickness sensors are employed in order to minimize the disturbance of the flow. The sensors consist of a light source (LED) and a photodiode a specified distance apart. The sensors rely on the change of the reflectivity at a liquid/vapor interface with the incidence angle of light as a result in the difference of index of refraction (Hurlburt 1996). The film thickness sensors have a sufficient response time for all test conditions and were calibrated from 0 to 3 millimeters. The film thickness sensors can indicate both film thickness and the location of the slug.

3. PHYSICAL OBSERVATIONS

Images and data from an experiment are presented to understand the qualitative characteristics of the flow. One test (300 milliliter slug, 207 kilopascal high side pressure, low side valve open) representative of the entire data range is shown.

3.1 Flow Visualization Images

Video images shown in Figure 2 show the progression of the slug and provide some insight to the physical phenomena occurring during the transient event. The camera is located 0.67 meters (66D) downstream of the first film thickness sensor. The flow is shown from right to left in the figure below.

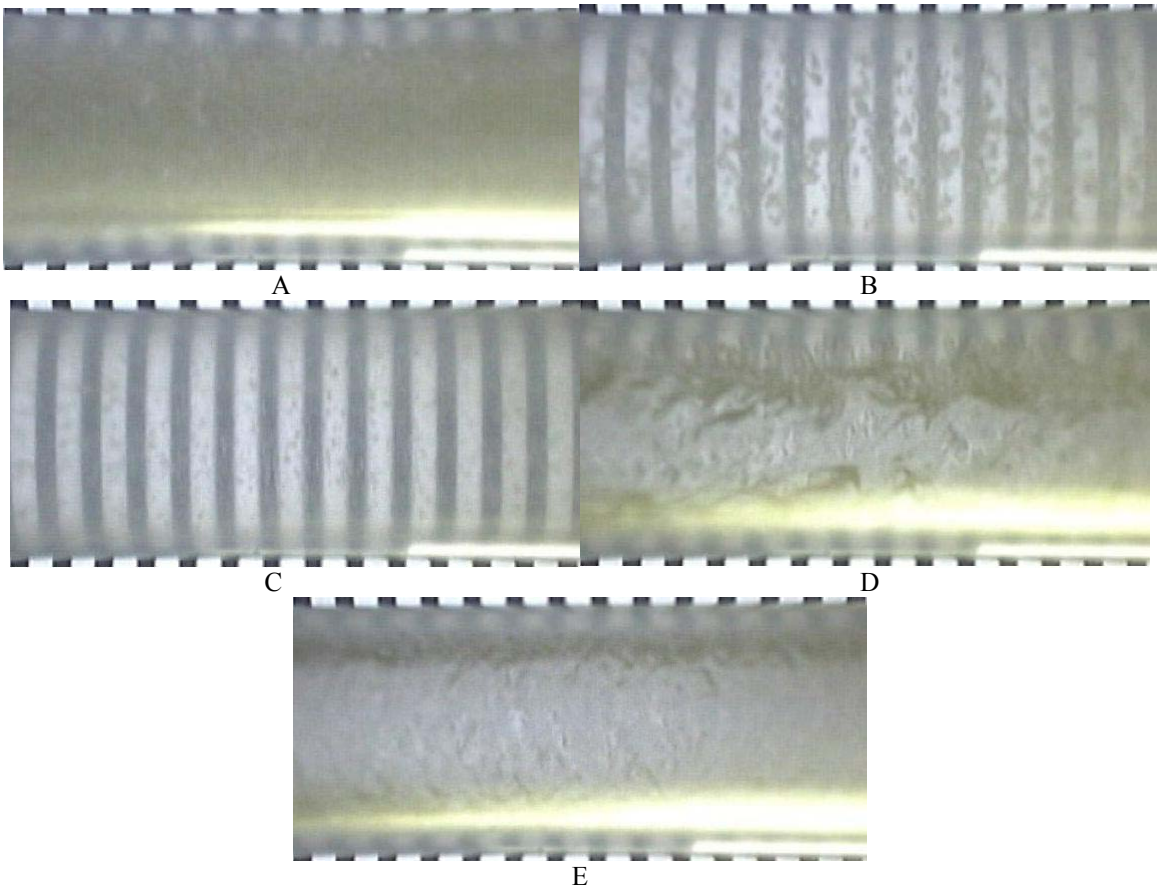

Figure 2: Flow Visualization Images (300 milliliter, 207 kilopascals, open valve test)

Figure 2A shows the leading edge of the slug. There is sufficient mixing of the air and water that there is no discernable interface. Within the front portion of the liquid slug, there is some penetration of the air, manifested by the bubbles shown in Figure 2B. In the center of the slug, there is no penetration of air; a complete slug of liquid is observed in Figure 2C. The slug flow then develops into an annular flow, leaving a film trailing behind. Figure 2D shows that there is an unsteady film following the trailing edge of the slug. A steady film of uniform thickness develops once the unsteadiness passes, shown in Figure 2E. These regions help describe and are consistent with data obtained from the film thickness sensors.

3.2 Film Thickness Information

Test data from the film thickness sensor at 0.5 meters from the zero location is shown in Figure 3.

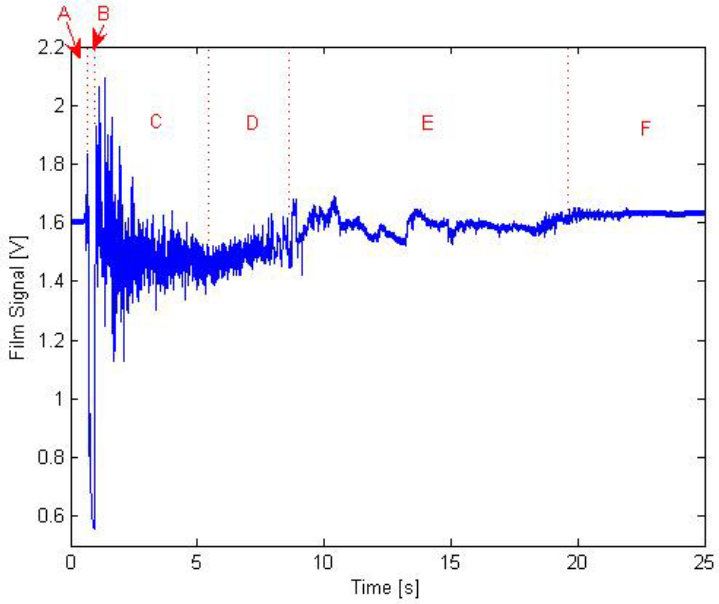

Figure 3: Film Thickness Voltage (300 milliliter, 207 kilopascals, open valve test)

Region A (0-0.5 seconds) in Figure 3 corresponds to the time that passes from the beginning of the test to when the film arrives at the film thickness sensor. The signal spikes indicating a non-zero film thickness: the leading edge of the slug appears to have liquid collecting near the bottom of the tube with air above it for a short period of time. The sensor indicates the presence of the slug in region B (0.5-0.8 seconds). The voltage drops significantly below that of the empty tube as expected due to the lack of a liquid/vapor interface to reflect.

The unsteady annular flow region mentioned in Figure 2D is also represented by region C (0.8-6 seconds). The high amplitude noise of the sensor indicates that the film is changing rapidly and unsteadily. The film thickness then stabilizes in region D (6-9 seconds); this corresponds to the image in Figure 2E. At the end of region D, the thin liquid film dissipates at the location of the film thickness sensor. Interestingly, the signal voltage increases upon the removal of the film. This is due to the difference in refraction index ratios between PVC/air and water/air interfaces.

The unsteadiness in region E (9-20 seconds) is the result of small droplets passing over the photodiode that have originated upstream from the sensor. The signal finally stabilizes in region F (20+ seconds) once all of the liquid droplets have passed.

3.3 Pressure Trends

The high side to low side pressure difference profile follows intuition. The pressure difference is zero, spikes to approximately the applied pressure while the slug is located between the transducers (207 kilopascals), then asymptotically moves back to zero slowly as the remaining film in the test section is dissipated.

4. ANALYTICAL MODELS

Three models have been applied to the experimental data in order to describe the dynamics of the slug motion: a mechanistic model, a film thickness model, and a viscous model. Again, one test (300 milliliter slug, 207 kilopascal high side pressure, low side valve open) representative of the entire data range is analyzed.

4.1 Mechanistic Model

The most simplistic, idealized model of the slug motion assumes the slug acts as one coherent mass that is accelerated by the pressure difference between the high side and the low side. The film thickness deposited on the wall and the viscosity of the liquid is not considered. The viscous pressure drop of the air is assumed constant and determined from steady operating conditions once the liquid film and slug have left the test section. Once these assumptions are applied, the acceleration is found from a simple force balance shown in equation (1).

$$a = \frac{\Delta pA}{\rho_L V_{Tot}} \tag{1}$$

The V indicated in the equation above refers to the volume that is known and inserted into the u-shaped portion of the test section, in this case 300 milliliters. This, of course, is grossly oversimplified, but does provide a first guess at the motion of the slug. It provides a basis for the development of the remaining models. The velocity and position can be determined by integrating the acceleration curve with time.

4.2 Film Thickness Model

The film thickness model considers the fact that the slug does not act as a coherent mass; it looses mass as a film is deposited on the wall. Also, the cross sectional area in which the pressure difference is applied is reduced due to the presence of a film. The averaged film thickness over the entire test section is calculated at each instant in time from the film thickness sensors. This film thickness is then multiplied by the circumference of the pipe and the length of the test section to determine the volume of the film. The slug volume is determined by subtracting the volume of the film from the total volume. The cross sectional area is similarly modified. The resulting acceleration is calculated in equation (2).

$$a = \frac{\Delta pA_F}{\rho_L V_S} \tag{2}$$

The viscosity is still not considered by this model and the film deposited in the u-shaped section of the tube is not taken into consideration. The model is, however, more realistic. It is interesting to note that the presence of a film would decrease the area, resulting in a decrease in the acceleration. At the same time, the volume of the slug is decreased, resulting in an increased acceleration. It is apparent from calculation and experimentation that including the film thickness results in a net increase in the acceleration.

4.3 Viscous Model

The viscous model takes the film thickness model developed from equation (2) and adds the viscous pressure drop associated with the liquid phase. The viscous pressure drop is proportional to the pipe length and dynamic pressure according to equation (3), where f is the friction factor.

$$\Delta p_V = f \frac{l_S}{D} \frac{\rho_L U^2}{2} \tag{3}$$

The slug length and diameter in equation (3) also change with time due to the averaged film thickness as described in the film thickness model. The flow is assumed to be completely turbulent and therefore the friction factor is calculated according to equation (4) for a smooth pipe (Colebrook 1939).

$$1/\sqrt{f} = -2.0\log\left(\frac{2.51}{\mathrm{Re}_D\sqrt{f}}\right) \tag{4}$$

The viscous pressure drop in equation (3) is then subtracted from the pressure difference used in equations (1) and (2) to generate the pressure difference applied to the slug. The acceleration in equation (5) determined from the viscous model is again, identical to that of the film thickness model except the pressure difference.

$$a = \frac{\Delta p_M A_F}{\rho_L V_S} \tag{5}$$

This model provides the most complication of the three considered.

5. EXPERIMENTAL RESULTS

The three models discussed above were applied to the data set referred to in the rest of the paper (300 milliliter slug, 207 kilopascal high side pressure, low side valve open). The acceleration calculations detailed in equations (1), (2), and (5) were computed in 0.001 second intervals; the data was taken at a rate of 1 kilohertz. The position curves shown in Figure 4 were generated by numerical integration of the acceleration.

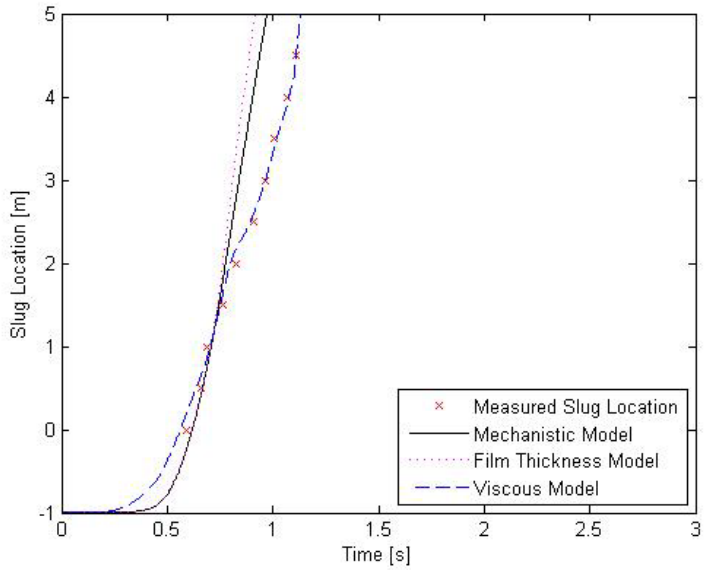

Figure 4: Slug Location in Time (300 milliliter, 207 kilopascals, open valve test)

The dynamic models begin at approximately -1 meters due to the fact that the slug is actually located approximately 1 meter downstream of the zero position (first film thickness sensor). The slug motion is quite interesting. The slug is accelerated very quickly at approximately 0.5 seconds and quickly reaches an almost steady velocity. As the velocity increases, the viscous pressure differences rapidly approach the driving pressure gradient.

The viscous model fits the observed slug location quite well. It, like the actual slug, accelerates more slowly than the more idealized models. The mechanistic and film thickness models still observe the same general trends as the data. This is expected, since the viscous model is the same model with slightly more complication. The two models deviate significantly from the observed behavior due to their continued acceleration resulting from a lack of a viscous drag force.

Additional complexities may be added to refine the model. Once such source will likely be work by Laurinat et. al. concerning pressure drop over a horizontal pipe in steady conditions and entrainment (Laurinat 1984). The viscous model, nonetheless, predicts the dynamic slug motion well.

6. CONCLUSIONS

A dynamical model of the slug motion should consider both the film thickness and viscous pressure drop associated with turbulent flow to be reasonably accurate. This model works well with air/water systems and should be used as a starting point when trying to understand slug motion during system startup for other refrigerants. The model is easy to implement, understand, and add complications to refine the accuracy of the motion prediction.

NOMENCLATURE

a	acceleration	[m/s^2]
A	cross-sectional area	[m^2]
A_F	film modified area	[m^2]
D	diameter	[m]
f	friction factor	[-]
l_S	slug length	[m]
Re_D	Reynolds number, diameter	[-]
U	slug velocity	[m/s]
V_{Tot}	total volume	[m^3]
V_S	slug volume	[m^3]
Δp	pressure difference	[Pa]
Δp_M	modified pressure difference	[Pa]
Δp_V	viscous pressure difference	[Pa]
ρ_L	liquid	[kg/m^3]

REFERENCES

Colebrook, C.F., 1939, Turbulent flow in Pipes with Particular Reference to the Transition Between the Smooth and Rough Pipe Laws, *Journal of the Institute of Civil Engineers London* , vol. 11.

Hurlburt, E.T. and Newell, T. A., 1996, Optical Film Thickness of Liquid Film Thickness and Wave Velocity in Liquid Film Flows, *Experiments in Fluids*, vol. 21, no. 5, p.357-362.

Jassim, E.W., Newell, T. A., and Chato, J. C., 2006, Probabilistic Determination of Two-Phase Flow Regimes Utilizing an Automated Image Recognition Technique, *International Refrigeration and Air Conditioning Conference at Purdue*, 2006, R010.

Laurinat, J.E., Hanratty, T. J., and Dallman, J. C., 1984, Pressure Drop and Film Height Measurements for Annular Gas-Liquid Flow, *Int. J. Multiphase Flow*, vol. 10., no. 3, p. 341-356.

ACKNOWLEDGEMENT

The authors appreciate the financial support of the Air Conditioning and Refrigeration Center at the University of Illinois.